Contribution from the Departments of Chemistry, The University of Michigan, Ann Arbor, Michigan 48109, and the University of Notre Dame, Notre Dame, Indiana 46556

Structure and Properties of an Unsymmetrically Substituted Six-Coordinate Iron(III) Porphyrin

KAREN M. ADAMS,[1a] PAUL G. RASMUSSEN,*[1a] W. ROBERT SCHEIDT,*[1b] and K. HATANO[1b]

Received November 9, 1978

The six-coordinate azido(pyridine)(tetraphenylporphinato)iron(III) complex, Fe(TPP)N_3py, has been prepared and its structure has been determined by diffraction techniques. The monoclinic unit cell contains four Fe(TPP)N_3py·$^1/_2$py formulations and has a = 14.519 (3) Å, b = 23.651 (5) Å, c = 13.030 (3) Å, and β = 103.94 (1)°. The space group is $P2_1/n$. The calculated and experimental densities are 1.28 and 1.27 g/cm^3 at 22 ± 1 °C. Diffracted intensities have been recorded for 4200 reflections classified as observed. The final discrepancy factors are R = 8.6% and R_w = 11.2%. The nearly tetragonal geometry and bond distances of the coordination group are consistent with a low-spin ferric ion. This spin state has been confirmed by a temperature-dependent magnetic analysis by using the Faraday method over the temperature range from 77 to 297 K. The effective magnetic moments range from 2.09 (1) μ_B at 77 K to 2.33 (1) μ_B at 297 K and are characteristic of a low spin state with spin–orbit coupling. Equilibrium constants for the addition of pyridine, *N*-methylimidazole, and imidazole to Fe(TPP)N_3 in CH_2Cl_2 at 23 ± 1 °C have been determined from the visible spectra. The equilibrium observed is Fe(TPP)N_3 + B (K_1) ⇄ Fe(TPP)N_3B where the product is six-coordinate. K_1 for pyridine is small, confirming the instability observed for Fe(TPP)N_3py in the magnetic study. For imidazole, Fe(TPP)N_3 + 2B (β_2) ⇄ Fe(TPP)$B_2^+N_3^-$ is observed in addition to the other equilibrium.

Introduction

Iron porphyrins and their reactions have been the subject of extensive research.[2,3] The interest in iron porphyrins stems not only from the diverse biological roles of the iron porphyrin moiety found in proteins, cytochromes, peroxidases, etc. but also from the array of physical properties observed for the coordinated Fe(II) and Fe(III) ions. Synthetic model complexes have been widely studied with the hope of clarifying the details of the many biological mechanisms involving iron porphyrin centers.

The compound described in this study, azido(pyridine)-(tetraphenylporphinato)iron(III), Fe(TPP)N_3py, is one of the very few synthetic ferric porphyrins with axial ligands that are not identical,[4,5] and the first for which an X-ray crystal structure has been completed. Azide and pyridine are the axial ligands in this complex. In this report we describe the stereochemistry of Fe(TPP)N_3py, the ferric ion spin state, and the equilibrium reaction of azido(tetraphenylporphinato)-iron(III), Fe(TPP)N_3, with pyridine, *N*-methylimidazole, and imidazole. The systematic study of Fe(TPP)N_3 with the selected bases offers information about the nature of nonidentical axial bonds and the trans effect of the ligands on each other. The unusual feature of the nonidentical axial ligands in this complex contributes new information about iron porphyrins.

Experimental Section

Syntheses. The starting iron porphyrin was chloro(tetraphenylporphinato)iron(III), Fe(TPP)Cl, and had been prepared by published methods.[6] All other chemicals were reagent grade. All solvents were dried according to standard procedures.[7]

About 100 mg of Fe(TPP)Cl was dissolved in 50 mL of chloroform. Into 15 mL of distilled water was dissolved 0.7 g of NaN_3, and the solution was made acidic with concentrated H_2SO_4. *Caution*! The hydrazoic acid, HN_3, generated is highly toxic and can be explosive outside of the aqueous solution! The chloroform solution was stirred together with the aqueous solution for 18 h. The chloroform solution was then separated, dried over anhydrous Na_2SO_4, and gravity filtered. The solvent was removed from the product Fe(TPP)N_3 under vacuum. The Fe(TPP)N_3 was recrystallized from either methylene chloride or benzene by allowing pentane to diffuse into the solution in a closed container. Dry solvents were used to minimize contamination with the hydrolysis product $[(Fe(TPP)]_2O$. Crystals of the final product, found later by X-ray crystallography to be the pyridine solvate Fe(TPP)N_3py·$^1/_2$py, were grown by dissolving Fe(TPP)N_3 in dry pyridine and allowing dry pentane to diffuse into the solution in a closed container.

Magnetic Study. The Faraday method was used for the magnetic analysis of Fe(TPP)N_3py·$^1/_2$py. A description of the Faraday apparatus used for this study, the procedure for data collection, and the documentation of the apparatus have been reported elsewhere.[8] The temperature range of the data is 77 K to room temperature. A $HgCo(SCN)_4$ standard was checked against the $Ni(NH_4)_2(SO_4)_2·6H_2O$ standard systematically throughout the data collections.

Initial measurements on several samples of Fe(TPP)N_3py·$^1/_2$py gave magnetic moments in the intermediate spin range, which were not reproducible from sample to sample. Characterization of these samples gave accurate C, H, and N analyses prior to the data collection. The infrared spectrum (Perkin-Elmer 457) on a KBr pellet showed two azide stretching frequencies, 2000 and 2040 cm^{-1}. The band at 2040 cm^{-1} corresponds to the high-spin compound Fe(TPP)N_3. The apparent loss of pyridine ligand demanded special precautions to obtain a homogeneous sample.

Crystals of the sample used for the magnetic study were selected under a microscope to ensure homogeneity. The crystals were not ground prior to data collection in order to reduce pyridine loss. (Replicate samples measured at room temperature indicated negligible error due to preferred orientation of the relatively large crystals.) For the low-temperature measurements, carried out in a helium atmosphere, the procedure for loading the sample avoided subjecting it to vacuum. The purity of the bulk sample used in the magnetic study was established from (1) the room temperature μ_{eff} of 2.33 (1) μ_B, a reasonable value for low-spin iron(III), (2) the spot quality of X-ray diffraction photographs, and (3) elemental analysis. Anal. Calcd for $C_{51.5}H_{35.5}N_{8.5}Fe$ (i.e., Fe(TPP)N_3py·$^1/_2$py): C, 74.59; H, 4.3; N, 14.36. Found: C, 74.57; H, 4.34; N, 14.28.

Equilibrium Study. The Fe(TPP)N_3 was prepared from the chloride derivative Fe(TPP)Cl as described above. Analytical grade methylene chloride (Mallinckrodt) was dried by reflux over phosphorus pentoxide followed by distillation. The pyridine (Mallinckrodt) and *N*-methylimidazole (Aldrich) were dried over potassium hydroxide for several days followed by reflux over barium oxide and distillation. The imidazole (Aldrich) was recrystallized twice from distilled benzene and dried under vacuum. Anal. Calcd for $C_{44}H_{28}N_7Fe$: C, 74.36; H, 3.97; N, 13.80. Found: C, 74.30; H, 4.01; N, 13.70.

A Cary 14 spectrometer was used for spectral measurements from 4600 to 7200 Å. The spectra were recorded at 23 ± 0.5 °C with a 1-cm path length cell. The equilibrium constants were determined from changes in the visible spectrum caused by varying the amine concentration in solutions with a prepared initial concentration of ~7 × 10^{-5} M Fe(TPP)N_3 in methylene chloride.

Crystal Structure Determination. Opaque black-violet crystals of Fe(TPP)N_3py·$^1/_2$py used for the X-ray structure determination were grown by slow evaporation from a 1:1 pyridine–chloroform solution of Fe(TPP)N_3. Precession photographs taken with Ni-filtered Cu Kα radiation uniquely determined the space group $P2_1/n$. Refined lattice parameters obtained during the data collection were a = 14.519 (3) Å, b = 23.651 (5) Å, c = 13.030 (3) Å, and β = 103.94 (1)°. The density measured by flotation in a mixture of CCl_4 and hexane was 1.28 (1) g/cm^3; calculated density for Fe(TPP)N_3py·$^1/_2$py was

0020-1669/79/1318-1892$01.00/0

1.27 g/cm^3, assuming one formula weight per asymmetric unit and $Z = 4$.

The intensity data were collected by using a Syntex $P1$ four-circle diffractometer. Graphite-monochromated Mo Kα radiation (α_1 = 0.709 24 Å, α_2 = 0.713 54 Å) was employed with a takeoff angle of approximately 4°. The θ–2θ scan technique was used with variable scan rates from 1.0 to 6.0°/min. The 2θ scan range was from 0.8° below Kα_1 to 0.8° above Kα_2. Backgrounds were measured from a time equal to half the scan time. All reflections for $(\sin\theta)/\lambda$ less than 0.602 Å^{-1} were scanned. Maximum possible hkl values were set at 19,32,17; minimum ones were set at −19,0,0. The intensities of four standard reflections were measured every 50 reflections. A least-squares fitting of the average relative intensity vs. exposure hours for the standards gave zero slope. Maximum deviation from the average relative intensity was 6%.

The raw intensity data were reduced[9] directly to a set of relative squared amplitudes, $|F_o|^2$, by application of the standard Lorentz and polarization factors. Standard deviations were calculated from[10] $\sigma^2(F_o) = [Ct + k^2B + p^2(Ct - kB)^2]/4|F_o|^2(Lp)^2$, where Ct is the count of the scan, k is the ratio of scanning time to background counting time, B is total background count, p is Ibers' factor[11] with a value of 0.04, and Lp is Lorentz and polarization factors. No absorption correction was made. The crystal size was 0.15 × 0.24 × 0.47 mm. The maximum and minimum transmission factors, 0.94 and 0.91, respectively, were calculated on the basis of a linear absorption coefficient of μ = 4.07 cm^{-1}. All systematically extinct reflections had very low counts ($F_o < 3\sigma(F_o)$), and when they were excluded from the data set, 7548 reflections were left. All reflections having F_o greater than $3\sigma(F_o)$ were flagged as observed, giving 4200 observed. Only observed reflections were used in the structure solution and refinement.

An origin-removed Patterson map was calculated[12] and the general position of the Fe atom was located at $2x$ = 0.194, $2y$ = 0.403, and $2z$ = 0.700. A series of difference Fourier maps, phased initially with the Fe atom, revealed the positions of all the carbon and nitrogen atoms in the axially coordinated pyridine and azide, and in the tetraphenylporphyrin group. Scattering factors for Fe, C, and N were taken from ref 13; anomalous scattering factors for Fe were taken from ref 14. After two cycles of block-diagonal least-squares refinement,[15] a difference Fourier map revealed electron density about the special position of rank two, whose coordinates are $^1/_2$, 0, 0 and 0, $^1/_2$, $^1/_2$. This electron density was assumed to be a disordered pyridine solvate. The formulation per asymmetric unit is thus Fe(TPP)N_3py·$^1/_2$py. This formula gives a calculated density of 1.268 g/cm^3 in good agreement with the experimental value of 1.28 g/cm^3. Since distinct peaks about $^1/_2$, 0, 0 could not be picked out in a way which made chemical sense, positions for carbon atoms of a "benzene" ring with C–C distances of 1.395 Å and occupancy factors of 0.5 were added in the solvent area. Refinement was continued by using full-matrix techniques with the phenyl rings and the disordered solvate held as rigid groups. Refinement was stopped when no shifts were greater than ~10% of the standard deviation for positions and none were greater than ~30% for thermal parameters. The hydrogen atoms, except for those of the solvate, were put in at fixed positions, with d(C–H) = 0.95 Å.[16] Their thermal parameters were fixed at one unit higher than the bonded carbon atom, i.e., Iso(H) = Iso(C) + 1. Scattering factors for H were taken from ref 17. With 33 hydrogens included, the iron, nitrogen, and carbon atoms and groups were refined again. The hydrogens were readjusted to the 0.95 Å C–H distance and the other atoms refined again. This process was repeated for three refinement cycles. The R values were constant for the last two cycles at $R = \sum||F_o| - |F_c||/\sum|F_o|$ = 8.6% and $R_w = \{\sum w(|F_o| - |F_c|)^2/\sum w|F_o|^2\}^{1/2}$ = 11.2% where F_o is the observed structure factor, F_c is the calculated structure factor, and w is the weighting factor, $w = 4F_o^2/\sigma^2(F_o)$. The final data to parameter ratio was 11.6. The average deviation of an observation of unit weight was 2.94. A final difference Fourier map showed the highest peak of 0.89 e/Å^3 located in the area of the phenyl rings. Atomic positional and thermal parameters are listed in Tables I, II, III, IV, and V. The relatively high R values result from difficulties due to the disordered solvent molecule and crystal quality generally. Attempts to obtain a better data set failed although the effort included sealing crystals into a capillary tube under pyridine.

Results and Discussion

Description of the Stereochemistry and Correlation with Spin State. The calculated bond lengths and bond angles for Fe(TPP)N_3py·$^1/_2$py are listed in Tables VI and VII. Figure 1 is a computer-drawn diagram[18] of the molecule. Figure 2 shows the packing in the unit cell. Figure 3 gives the displacements of the atoms from the mean skeletal plane.

Table I. Fractional Atomic Coordinates of Porphinato Core and Axial Ligands[a]

atom[b]	x	y	z
Fe	0.1046 (1)	0.2005 (0)	0.3503 (1)
N_1	0.0484 (4)	0.1351 (2)	0.2596 (4)
N_2	0.1727 (4)	0.2225 (2)	0.2413 (4)
N_3	0.1567 (4)	0.2674 (2)	0.4372 (4)
N_4	0.0334 (4)	0.1800 (2)	0.4572 (4)
N_5	0.2092 (5)	0.1558 (3)	0.4280 (5)
N_6	−0.0098 (5)	0.2504 (3)	0.2728 (5)
N_{51}	0.2577 (8)	0.1271 (4)	0.3909 (7)
N_{52}	0.2966 (10)	0.0982 (6)	0.3488 (12)
C_6	−0.0497 (7)	0.2885 (4)	0.3239 (7)
C_7	−0.1218 (8)	0.3221 (5)	0.2770 (9)
C_8	−0.1577 (8)	0.3168 (5)	0.1687 (9)
C_9	−0.1190 (8)	0.2792 (5)	0.1153 (8)
C_{10}	−0.0450 (7)	0.2464 (4)	0.1673 (6)
C_{11}	0.0698 (5)	0.1174 (3)	0.1689 (5)
C_{12}	0.1398 (6)	0.1397 (3)	0.1252 (6)
C_{13}	0.1864 (5)	0.1899 (3)	0.1591 (6)
C_{14}	0.2505 (6)	0.2182 (4)	0.1083 (6)
C_{15}	0.2711 (6)	0.2687 (4)	0.1554 (7)
C_{16}	0.2234 (6)	0.2712 (3)	0.2409 (6)
C_{17}	0.2322 (6)	0.3155 (3)	0.3120 (6)
C_{18}	0.2039 (6)	0.3128 (3)	0.4048 (6)
C_{19}	0.2236 (7)	0.3554 (3)	0.4865 (6)
C_{20}	0.1884 (7)	0.3360 (4)	0.5668 (6)
C_{21}	0.1473 (6)	0.2814 (3)	0.5371 (6)
C_{22}	0.0969 (6)	0.2497 (3)	0.5959 (6)
C_{23}	0.0446 (5)	0.2018 (3)	0.5580 (6)
C_{24}	−0.0087 (6)	0.1689 (3)	0.6149 (6)
C_{25}	−0.0556 (6)	0.1294 (3)	0.5498 (6)
C_{26}	−0.0293 (5)	0.1352 (3)	0.4507 (6)
C_{27}	−0.0608 (5)	0.1001 (3)	0.3637 (6)
C_{28}	−0.0260 (5)	0.1008 (3)	0.2731 (5)
C_{29}	−0.0516 (6)	0.0635 (3)	0.1871 (6)
C_{30}	0.0062 (6)	0.0724 (3)	0.1228 (6)

[a] Standard deviation in parentheses. [b] N_1 through N_4 and C_{11} through C_{30} make up the porphinato core. N_5, N_{51}, and N_{52} are the azide nitrogens; N_5 is bonded to the Fe. N_6 and C_6 through C_{10} are the atoms of the pyridine ligand.

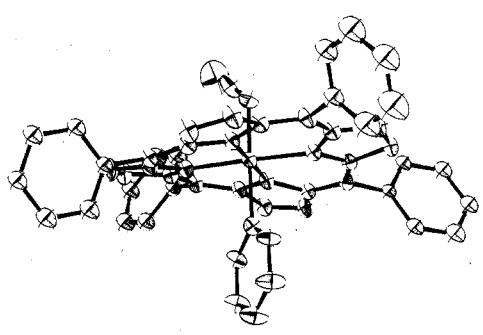

Figure 1. Perspective drawing of Fe(TPP)N_3py; 50% probability ellipsoids. Hydrogens have been omitted for clarity.

The molecule has no space group required symmetry, but Figures 1 and 3 qualitatively show the quasi-S_4 ruffling[19] of the porphinato skeleton. This symmetry is most easily seen in the methine carbons. Their displacements alternate above and below the mean porphyrin plane. This quasi-S_4 ruffling is also exemplified in the dihedral angles of the pyrrole rings with the mean plane of the porphinato core. These are listed in Table VIII. Similar magnitudes in quasi-S_4 ruffling are observed, for example, in bis(imidazole)(tetraphenylporphinato)iron(III) chloride,[20] which also has no required space group symmetry. When little or no symmetry is required of the metalloporphyrin in its crystalline arrangement, it is generally observed that the mean deviation from the average

Table II. Anisotropic Thermal Parameters (in Å^2)[a]

	U_{11}	U_{22}	U_{33}	U_{12}	U_{13}	U_{23}
Fe	0.0057 (1)	0.0014 (0)	0.0048 (1)	−0.0004 (0)	0.0013 (1)	−0.0002 (0)
N_1	0.0060 (4)	0.0014 (1)	0.0049 (4)	−0.0003 (2)	0.0020 (3)	−0.0004 (2)
N_2	0.0059 (4)	0.0013 (1)	0.0049 (4)	−0.0007 (2)	0.0016 (3)	−0.0004 (2)
N_3	0.0063 (4)	0.0013 (1)	0.0050 (4)	−0.0005 (2)	0.0009 (3)	−0.0003 (2)
N_4	0.0053 (4)	0.0014 (1)	0.0054 (4)	−0.0002 (2)	0.0013 (3)	−0.0002 (2)
N_5	0.0075 (5)	0.0022 (2)	0.0067 (5)	0.0005 (2)	0.0015 (4)	−0.0003 (2)
N_6	0.0064 (4)	0.0018 (1)	0.0064 (5)	0.0001 (2)	0.0016 (4)	−0.0002 (2)
N_{51}	0.0132 (9)	0.0022 (2)	0.0093 (7)	0.0002 (3)	0.0035 (6)	0.0009 (3)
N_{52}	0.0205 (14)	0.0045 (4)	0.0255 (17)	0.0037 (6)	0.0123 (13)	0.0002 (6)
C_6	0.0075 (6)	0.0025 (2)	0.0076 (7)	0.0015 (3)	0.0000 (5)	−0.0003 (3)
C_7	0.0100 (8)	0.0034 (3)	0.0127 (11)	0.0024 (4)	0.0008 (8)	−0.0007 (4)
C_8	0.0108 (9)	0.0031 (3)	0.0106 (10)	0.0023 (4)	−0.0002 (7)	0.0005 (4)
C_9	0.0098 (8)	0.0029 (2)	0.0084 (8)	0.0009 (4)	−0.0007 (7)	0.0001 (4)
C_{10}	0.0083 (7)	0.0023 (2)	0.0058 (6)	0.0003 (3)	0.0005 (5)	0.0003 (3)
C_{11}	0.0061 (5)	0.0015 (2)	0.0047 (5)	−0.0003 (2)	0.0018 (4)	−0.0000 (2)
C_{12}	0.0068 (5)	0.0016 (2)	0.0054 (5)	−0.0004 (2)	0.0020 (4)	−0.0004 (2)
C_{13}	0.0063 (5)	0.0016 (2)	0.0057 (5)	−0.0004 (2)	0.0017 (4)	−0.0004 (2)
C_{14}	0.0079 (6)	0.0021 (2)	0.0075 (7)	−0.0011 (3)	0.0032 (5)	−0.0007 (3)
C_{15}	0.0080 (6)	0.0021 (2)	0.0077 (7)	−0.0017 (3)	0.0025 (5)	−0.0006 (3)
C_{16}	0.0063 (5)	0.0018 (2)	0.0059 (6)	−0.0006 (3)	0.0014 (5)	0.0000 (3)
C_{17}	0.0070 (5)	0.0015 (2)	0.0055 (6)	−0.0006 (2)	0.0013 (4)	−0.0003 (2)
C_{18}	0.0066 (5)	0.0016 (2)	0.0066 (6)	−0.0005 (2)	0.0013 (5)	−0.0005 (3)
C_{19}	0.0107 (7)	0.0017 (2)	0.0067 (6)	−0.0013 (3)	0.0027 (6)	−0.0009 (3)
C_{20}	0.0102 (7)	0.0020 (2)	0.0058 (6)	−0.0011 (3)	0.0020 (5)	−0.0009 (3)
C_{21}	0.0068 (6)	0.0016 (2)	0.0054 (6)	−0.0007 (2)	0.0002 (5)	−0.0006 (2)
C_{22}	0.0082 (6)	0.0019 (2)	0.0050 (5)	−0.0005 (3)	0.0018 (5)	−0.0006 (3)
C_{23}	0.0064 (5)	0.0017 (2)	0.0056 (5)	−0.0003 (3)	0.0016 (4)	−0.0004 (3)
C_{24}	0.0082 (6)	0.0020 (2)	0.0056 (6)	−0.0004 (3)	0.0031 (5)	−0.0005 (3)
C_{25}	0.0072 (6)	0.0019 (2)	0.0065 (6)	−0.0004 (3)	0.0031 (5)	0.0001 (3)
C_{26}	0.0053 (5)	0.0015 (2)	0.0062 (6)	−0.0000 (2)	0.0017 (4)	−0.0001 (2)
C_{27}	0.0049 (5)	0.0013 (1)	0.0065 (6)	−0.0003 (2)	0.0013 (4)	0.0001 (2)
C_{28}	0.0053 (5)	0.0013 (1)	0.0052 (5)	−0.0002 (2)	0.0014 (4)	−0.0003 (2)
C_{29}	0.0067 (5)	0.0015 (2)	0.0062 (6)	−0.0008 (2)	0.0018 (5)	−0.0002 (2)
C_{30}	0.0068 (5)	0.0016 (2)	0.0060 (6)	−0.0007 (2)	0.0014 (5)	−0.0004 (2)

[a] In the form of $\exp[-2\pi^2(h^2a^{*2}U_{11} + \ldots + 2hka^*b^*U_{12} + \ldots)]$; standard deviations are in parentheses.

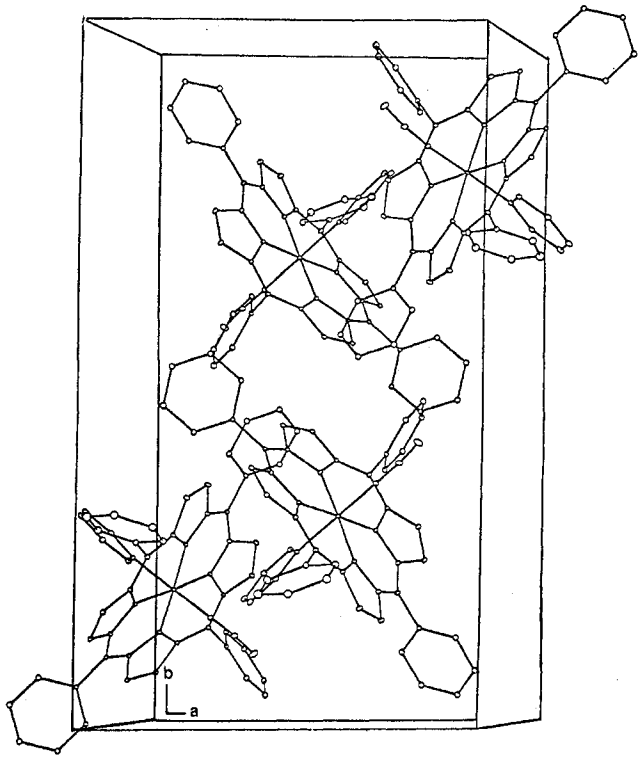

Figure 2. Porphyrin packing within the unit cell.

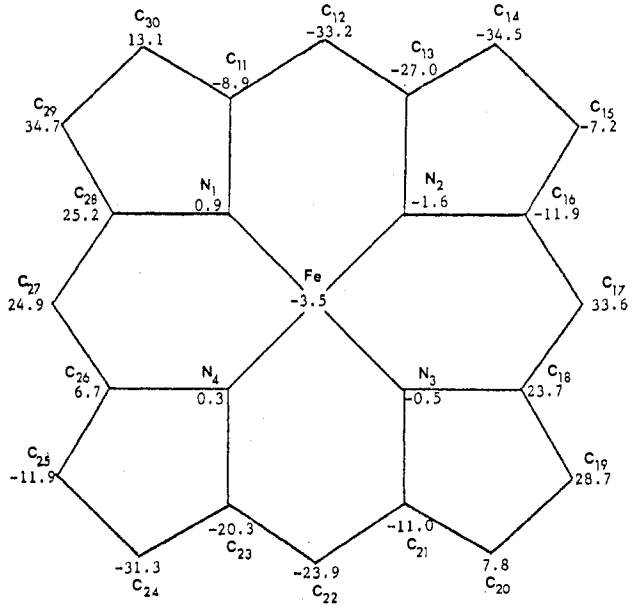

Figure 3. Diagram of porphinato core showing the perpendicular displacements from the mean plane. The units are 0.01 Å. Negative displacements are toward the azide.

bond length or bond angle of the class differs insignificantly from the root-mean-square estimated standard deviation.[19] These data have been tabulated in Table IX. In these circumstances, the symmetry of the porphyrin core can be raised to quasi-D_{2d}.[19]

The average length of the four iron–porphinato nitrogen bonds in $Fe(TPP)N_3py\cdot{}^1/_2py$ is $Fe-N_p$ = 1.989 (6, 5) Å. In low-spin ferric porphyrins, the iron atom is six-coordinate and coplanar with the porphinato nitrogens.[1] The chloride derivative[20] of $Fe(TPP)(Im)_2^+$ and the perchlorate derivative[21] of $Fe(OEP)(Im)_2^+$ are the only synthetic low-spin ferric porphyrins for which crystal structure determinations have been done. An $Fe-N_p$ bond length of 1.99 Å is also observed

Table III. Phenyl Parameters:[a] Group, Atomic, and Thermal

group[b]	x	y	z	
Ph_{120}	0.1651 (4)	0.1090 (2)	0.0342 (4)	
Ph_{170}	0.2750 (4)	0.3693 (2)	0.2833 (4)	
Ph_{220}	0.0944 (6)	0.2710 (3)	0.7029 (5)	
Ph_{270}	−0.1342 (3)	0.0563 (2)	0.3693 (4)	
phenyl carbon[c]	x	y	z	B,[d] Å^2
C_{121}	0.1651	0.1090	0.0342	4.3 (2)
C_{122}	0.2175	0.0591	0.0563	6.2 (2)
C_{123}	0.2470	0.0310	−0.0243	7.1 (2)
C_{124}	0.2242	0.0527	−0.1269	6.2 (2)
C_{125}	0.1718	0.1025	−0.1489	6.5 (2)
C_{126}	0.1423	0.1307	−0.0683	5.3 (2)
C_{171}	0.2750	0.3693	0.2833	4.4 (2)
C_{172}	0.3685	0.3843	0.3309	5.5 (2)
C_{173}	0.4067	0.4341	0.3013	5.9 (2)
C_{174}	0.3514	0.4690	0.2242	6.0 (2)
C_{175}	0.2579	0.4540	0.1767	6.8 (2)
C_{176}	0.2197	0.4042	0.2062	6.3 (2)
C_{221}	0.0944	0.2710	0.7029	6.1 (2)
C_{222}	0.1773	0.2717	0.7836	8.0 (3)
C_{223}	0.1752	0.2915	0.8838	11.1 (4)
C_{224}	0.0901	0.3106	0.9034	11.4 (4)
C_{225}	0.0072	0.3100	0.8226	14.1 (5)
C_{226}	0.0093	0.2902	0.7224	11.0 (4)
C_{271}	−0.1343	0.0563	0.3693	3.8 (2)
C_{272}	−0.2288	0.0723	0.3570	5.6 (2)
C_{273}	−0.2956	0.0327	0.3720	6.8 (2)
C_{274}	−0.2678	−0.0229	0.3992	6.0 (2)
C_{275}	−0.1733	−0.0388	0.4116	5.8 (2)
C_{276}	−0.1065	0.0008	0.3966	4.6 (2)

[a] Standard deviations in parentheses. [b] The phenyl group parameters are the fractional positions, x, y, z, of the centroid of the six-membered ring. [c] The phenyl carbons of the six-membered ring are numbered such that C_{xx1} is attached to C_{xx} of the porphinato core; the other carbons are numbered in succession. [d] Isotropic temperature factor is in the form $\exp\{-(B/4)[(2 \sin\theta)^2/\lambda]\}$.

Table IV. Disordered Solvent Parameters[a]

group centroid	x	y	z		
Ph_{50}	0.491 (2)	−0.015 (2)	−0.027 (2)		
carbon atoms	x	y	z	B, Å^2	multiplicity
C_{51}	0.4911	−0.0159	−0.0272	20	0.5
C_{52}	0.5085	−0.0653	−0.0780	20	0.5
C_{53}	0.5356	−0.0621	−0.1735	20	0.5
C_{54}	0.5454	−0.0095	−0.2182	20	0.5
C_{55}	0.5280	0.0399	−0.1674	20	0.5
C_{56}	0.5009	0.0367	−0.0719	20	0.5

[a] Standard deviations in parentheses. [b] Group parameters defined in Table III. [c] The solvent molecule was given a fixed group thermal parameter of 20.

in the bis(imidazole) complex.[20] In $Fe(TPP)(Im)_2^+$ and $Fe(TPP)N_3py$, the iron atom is essentially coplanar with the porphinato nitrogen atoms. These equatorial parameters appear to be consistent with the absence of an unpaired electron in the $d_{x^2-y^2}$ orbital.[2]

The axial bond length of the iron to the azide nitrogen is $Fe-N_{az}$ = 1.925 (7) Å; the Fe–N–N angle is 125.6 (7)°. The projection of the azide ligand onto the porphinato plane makes angles of approximately 40 and 50° with adjacent $Fe-N_p$ vectors. The plane of the pyridine ligand is nearly perpendicular to the plane of the porphyrin (89°). The projection of the pyridine ligand onto the porphyrin plane again results in angles of approximately 40 and 50° with adjacent $Fe-N_p$ vectors. The angle between the azide projection and the pyridine projection is approximately 10°.

Table V. Fractional Atomic Coordinates for Hydrogen Atoms[a]

atom[a]	x	y	z
H_6	−0.0251	0.2924	0.3979
H_7	−0.1485	0.3483	0.3158
H_8	−0.2093	0.3400	0.1340
H_9	−0.1434	0.2754	0.0406
H_{10}	−0.0177	0.2201	0.1287
H_{14}	0.2736	0.2040	0.0519
H_{15}	0.3099	0.2970	0.1362
H_{19}	0.2551	0.3902	0.4841
H_{20}	0.1910	0.3540	0.6319
H_{24}	−0.0110	0.1742	0.6864
H_{25}	−0.0984	0.1022	0.5658
H_{29}	−0.1014	0.0365	0.1762
H_{30}	0.0053	0.0530	0.0590
H_{122}	0.2329	0.0444	0.1263
H_{123}	0.2831	−0.0028	−0.0090
H_{124}	0.2449	0.0338	−0.1814
H_{125}	0.1568	0.1175	−0.2185
H_{126}	0.1066	0.1647	−0.0833
H_{172}	0.4061	0.3604	0.3838
H_{173}	0.4704	0.4440	0.3340
H_{174}	0.3776	0.5026	0.2043
H_{175}	0.2205	0.4776	0.1243
H_{176}	0.1562	0.3939	0.1741
H_{222}	0.2351	0.2586	0.7702
H_{223}	0.2317	0.2920	0.9388
H_{224}	0.0887	0.3241	0.9716
H_{225}	−0.0507	0.3229	0.8360
H_{226}	−0.0472	0.2896	0.6674
H_{272}	−0.2477	0.1101	0.3385
H_{273}	−0.3599	0.0435	0.3638
H_{274}	−0.3132	−0.0498	0.4098
H_{275}	−0.1544	−0.0766	0.4305
H_{276}	−0.0422	−0.0101	0.4051

[a] The label number for a hydrogen is identical with the number for the carbon to which it is attached.

Table VI. Bond Lengths in Coordination Group and Porphinato Skeleton[a]

type[b]	length, Å	type[b]	length, Å	type[b]	length, Å
$Fe-N_1$	1.999 (6)	N_p-C_a		C_a-C_b	
$Fe-N_2$	1.985 (6)	N_1-C_{11}	1.358 (8)	$C_{11}-C_{30}$	1.442 (10)
$Fe-N_3$	1.986 (6)	N_1-C_{28}	1.395 (8)	$C_{13}-C_{14}$	1.432 (11)
$Fe-N_4$	1.985 (6)	N_2-C_{13}	1.373 (9)	$C_{16}-C_{15}$	1.448 (11)
$Fe-N_5$	1.925 (7)	N_2-C_{16}	1.368 (9)	$C_{18}-C_{19}$	1.443 (10)
$Fe-N_6$	2.089 (6)	N_3-C_{18}	1.394 (9)	$C_{21}-C_{20}$	1.436 (10)
N_5-N_{51}	1.164 (11)	N_3-C_{21}	1.381 (9)	$C_{23}-C_{24}$	1.423 (11)
$N_{51}-N_{52}$	1.111 (12)	N_4-C_{23}	1.383 (9)	$C_{26}-C_{25}$	1.437 (10)
N_6-C_6	1.333 (10)	N_4-C_{26}	1.387 (9)	$C_{28}-C_{29}$	1.406 (9)
C_6-C_7	1.338 (12)	C_m-C_a		C_b-C_b	
C_7-C_8	1.387 (14)	$C_{12}-C_{11}$	1.384 (10)	$C_{14}-C_{15}$	1.343 (11)
C_8-C_9	1.333 (14)	$C_{12}-C_{13}$	1.385 (10)	$C_{19}-C_{20}$	1.350 (11)
C_9-C_{10}	1.366 (12)	$C_{17}-C_{16}$	1.384 (10)	$C_{24}-C_{25}$	1.335 (10)
N_6-C_{10}	1.349 (10)	$C_{17}-C_{18}$	1.368 (10)	$C_{29}-C_{30}$	1.338 (10)
		$C_{22}-C_{21}$	1.400 (11)		
		$C_{22}-C_{23}$	1.386 (10)		
		$C_{27}-C_{26}$	1.391 (10)		
		$C_{27}-C_{28}$	1.391 (10)		

[a] Standard deviations in parentheses. [b] Atom types with alphabetical subscripts are defined as follows: N_p, porphinato nitrogens; C_a and C_b, α and β carbons of the porphyrin pyrrole; C_m, methine carbons of the porphyrin. Tables VII and IX also use this notation.

The axial $Fe-N_{az}$ bond length of 1.925 (7) Å is longer than the corresponding distance observed in the five-coordinate high-spin derivative $Fe(TPP)N_3$ (1.909 Å).[22] The other axial bond length ($Fe-N_{py}$) is 2.089 (6) Å, which is longer than the normal axial $Fe^{III}-N$ distance of 2.00 Å.[2,20] This lengthening is probably the result of steric interactions of the pyridine with the porphinato core. Distances between the α pyridine hydrogen atoms and the porphinato nitrogen atoms are $N_1\cdots H_{10}$ = 2.67 Å, $N_2\cdots H_{10}$ = 2.80 Å, $N_3\cdots H_6$ = 2.63 Å, and $N_4\cdots H_6$ = 2.84 Å. Lengthening of the axial Fe–N bonds has also been observed in $Fe^{II}(TPP)(pip)_2$.[23] The bis(piperidine)ferrous

Table VII. Bond Angles in Coordination Group and Porphinato Skeleton[a]

type	angle, deg	type	angle, deg	type	angle, deg
N_1FeN_2	89.0 (2)	$C_aN_pC_a$		$C_aC_bC_b$	
N_2FeN_3	90.7 (2)	$C_{28}N_1C_{11}$	106.2 (6)	$C_{13}C_{14}C_{15}$	107.7 (7)
N_3FeN_4	89.2 (2)	$C_{13}N_2C_{16}$	106.9 (6)	$C_{14}C_{15}C_{16}$	107.0 (7)
N_4FeN_1	91.0 (2)	$C_{18}N_3C_{21}$	105.5 (6)	$C_{18}C_{19}C_{20}$	106.8 (7)
N_1FeN_5	92.5 (3)	$C_{23}N_4C_{26}$	105.6 (6)	$C_{19}C_{20}C_{21}$	107.9 (7)
N_2FeN_5	93.1 (3)	FeN_pC_a		$C_{23}C_{24}C_{25}$	108.1 (7)
N_3FeN_5	89.7 (3)	FeN_1C_{28}	126.4 (4)	$C_{24}C_{25}C_{26}$	107.3 (7)
N_4FeN_5	88.6 (3)	FeN_1C_{11}	127.3 (5)	$C_{28}C_{29}C_{30}$	108.3 (7)
N_1FeN_6	89.3 (2)	FeN_2C_{13}	127.0 (5)	$C_{29}C_{30}C_{11}$	107.0 (7)
N_2FeN_6	88.9 (2)	FeN_2C_{16}	125.8 (5)	$C_mC_aC_b$	
N_3FeN_6	88.6 (2)	FeN_3C_{18}	126.1 (5)	$C_{30}C_{11}C_{12}$	124.8 (7)
N_4FeN_6	89.4 (2)	FeN_3C_{21}	128.2 (5)	$C_{12}C_{13}C_{14}$	125.2 (7)
N_5FeN_6	177.3 (3)	FeN_4C_{23}	127.8 (5)	$C_{15}C_{16}C_{17}$	124.2 (7)
FeN_5N_{51}	125.6 (7)	FeN_4C_{26}	126.1 (5)	$C_{17}C_{18}C_{19}$	124.8 (7)
$N_5N_{51}N_{52}$	173.6 (14)	$N_pC_aC_m$		$C_{20}C_{21}C_{22}$	125.0 (7)
FeN_6C_6	122.1 (5)	$N_1C_{28}C_{27}$	124.4 (6)	$C_{22}C_{23}C_{24}$	125.5 (7)
FeN_6C_{10}	121.0 (6)	$N_1C_{11}C_{12}$	125.9 (7)	$C_{25}C_{26}C_{27}$	124.6 (7)
$C_6C_7C_8$	118.1 (10)	$N_2C_{13}C_{12}$	125.3 (7)	$C_{27}C_{28}C_{29}$	126.0 (7)
$C_7C_8C_9$	119.3 (9)	$N_2C_{16}C_{17}$	126.7 (7)	$C_aC_mC_a$	
$C_8C_9C_{10}$	120.0 (9)	$N_3C_{18}C_{17}$	125.3 (7)	$C_{11}C_{12}C_{13}$	123.1 (7)
$C_9C_{10}N_6$	121.6 (8)	$N_3C_{21}C_{22}$	124.8 (6)	$C_{16}C_{17}C_{18}$	123.8 (7)
$N_6C_6C_7$	124.1 (8)	$N_4C_{23}C_{22}$	124.9 (7)	$C_{21}C_{22}C_{23}$	123.9 (7)
		$N_4C_{26}C_{27}$	126.0 (7)	$C_{26}C_{27}C_{28}$	124.7 (7)
		$N_pC_aC_b$			
		$N_1C_{28}C_{29}$	109.2 (6)		
		$N_1C_{11}C_{30}$	109.4 (6)		
		$N_2C_{13}C_{14}$	109.3 (6)		
		$N_2C_{16}C_{15}$	109.1 (6)		
		$N_3C_{18}C_{19}$	109.8 (7)		
		$N_3C_{21}C_{20}$	110.0 (7)		
		$N_4C_{23}C_{24}$	109.6 (7)		
		$N_4C_{26}C_{25}$	109.3 (6)		

[a] Standard deviations in parentheses.

Table VIII. Dihedral Angles of Least-Squares Planes

plane 1	plane 2	angle, deg
four porphinato nitrogens	phenyl 120	69
	phenyl 170	73
	phenyl 220	63
	phenyl 270	73
	N_1-pyrrole	11
	N_2-pyrrole	12
	N_3-pyrrole	11
	N_4-pyrrole	10
Fe,N_5,N_{51}	N_5,N_1,N_3	50
	N_5,N_2,N_4	39
pyridine	N_6,N_1N_3	40
	N_6,N_2,N_4	49

Table IX. Mean Bond Lengths (Å) for Chemically Equivalent Bonds in the Porphinato Core

type	mean[a]	type	mean[a]
$Fe-N_p$	1.989 (6, 5)	C_b-C_b	1.342 (11, 5)
N_p-C_a	1.380 (9, 10)	C_a-C_m	1.386 (10, 6)
C_a-C_b	1.433 (10, 10)		

[a] In parentheses are root-mean-square estimated standard deviation and average mean deviation, respectively.

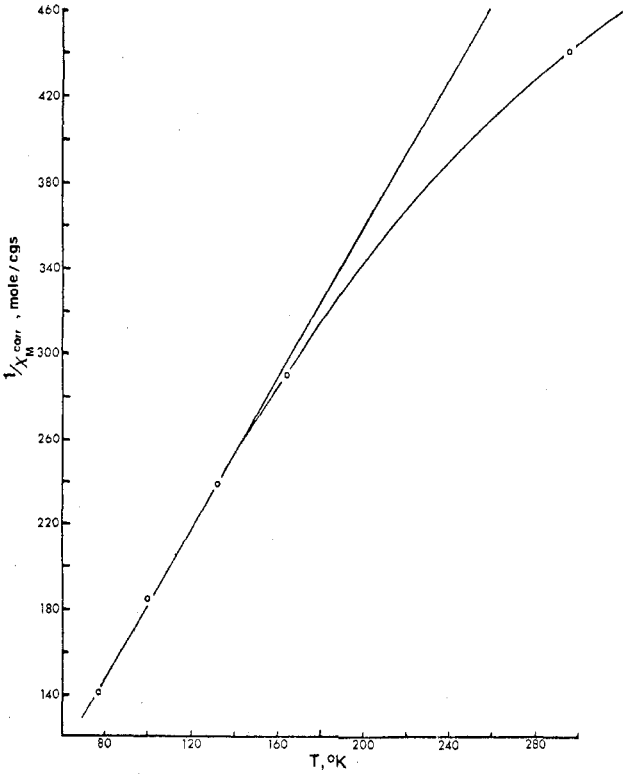

Figure 4. Plot of $1/\chi_M^{cor}$ vs. T for $Fe(TPP)N_3py\cdot{}^1/_2py$.

complex has been shown to be low spin even with the axial bonds lengthened to 2.126 Å. The axial bond lengths of low-spin $Co^{III}(TPP)(NO_2)(3,5\text{-lut})$[24] are interesting for comparison with $Fe(TPP)N_3py\cdot{}^1/_2py$. The $Co-N_{NO_2}$ bond length is 1.948 (4) Å; the $Co-N_{lut}$ bond length is 2.036 (4) Å. These are comparable to the axial bonds of $Fe(TPP)N_3py\cdot{}^1/_2py$ and reflect the absence of the unpaired electron in the d_{z^2} orbital of the Co(III) ion. The effect of the unpaired electron in the d_{z^2} orbital on the axial bond lengths can be seen in $[(pip)_2Co(TPP)]^+$[25] compared with the reduced species $(pip)_2Co(TPP)$.[26] The equatorial $Co-N_p$ bond lengths are almost identical in these two cobalt porphyrins. The axial lengths are $Co(III)-N_{pip}$ = 2.060 (3) Å and $Co(II)-N_{pip}$ = 2.436 (2) Å. Thus, the stereochemical parameters for $Fe(TPP)N_3py\cdot{}^1/_2py$ are consistent with a low-spin ferric ion that is described in the magnetic analysis which follows.

Temperature-Dependent Magnetic Analysis. Magnetic susceptibilities, χ, and moments, μ, for $Fe(TPP)N_3py\cdot{}^1/_2py$ from 77 K to room temperature are given in Table X. A plot

Table X. Temperature-Dependent Magnetic Data for $Fe(TTP)N_3py\cdot{}^1/_2py$

T,[a] K	χ_g,[b] cgs/g	χ_M^{cor},[b,c] cgs/mol	μ_{eff},[b,d] μ_B
77	7.93 (11) × 10^{-6}	7.08 (9) × 10^{-3}	2.09 (1)
100	5.88 (10) × 10^{-6}	5.37 (9) × 10^{-3}	2.07 (2)
132	4.45 (7) × 10^{-6}	4.19 (6) × 10^{-3}	2.10 (2)
164.5	3.56 (5) × 10^{-6}	3.45 (4) × 10^{-3}	2.14 (1)
297	2.15 (1) × 10^{-6}	2.28 (1) × 10^{-3}	2.33 (1)

[a] Temperatures are estimated to be accurate to ±1 K. [b] In parentheses are standard deviations for determinations at three field strengths. [c] χ_M^{cor} is the molar susceptibility corrected for diamagnetism. The diamagnetic correction used for TTP is -380×10^{-6} cgs/mol. [d] The effective magnetic moment, μ_{eff}, is defined as $2.83(\chi_M^{cor}T)^{1/2}$.

of $1/\chi_M^{cor}$ vs. T is shown in Figure 4. The Θ value, 4 (5) K has been calculated from a linear least-squares fit of this plot for the three lowest temperature data. This small Θ value is in agreement with Weiss constants reported for ferric porphyrins.[27,28] Since there is no short intermolecular separations of the iron atoms in $Fe(TPP)N_3py\cdot{}^1/_2py$, any substantial Θ value would probably be an indication of sample impurities.

The values of μ in Table X as well as their temperature dependence are typical for ferric ion with one unpaired electron,[29] i.e., the ^2T ground term of a ferric ion in a strong octahedral field. The theoretical magnetic moment of a ^2T ground term can be derived from Van Vleck's equation and is a complicated function of λ, the spin–orbit coupling constant, and T, temperature.[29,30] Thus, the magnetic moment of a ^2T ground term deviates from the spin-only value of 1.7 μ_B, $\mu = 2(S(S+1))^{1/2}$, and depends on temperature. Calculation of the magnetic moment of ferric ion in a strong octahedral field, by using the spin–orbit coupling constant of the free ion yields a μ of 2.4 μ_B at 300 K,[29] whereas experimental values for $K_3Fe(CN)_6$ are $\mu(80\text{ K}) = 1.90\ \mu_B$ and $\mu(300\text{ K}) = 2.25\ \mu_B$.[29] Although the ligand field of $Fe(TPP)N_3py$ is tetragonal, it can be considered a ^2T ground term split by an axially symmetric field.[30,31] The tetragonal field does not completely quench the spin–orbit coupling, so the magnetic moment will be a function of λ and T, as in the octahedral case, and also of the tetragonal splitting parameter.[30,31] The magnetic moments should reflect this with values higher than spin-only and behavior very similar to the octahedral case, consistent with our observations of $Fe(TPP)N_3py\cdot{}^1/_2py$.

Equilibrium Study. In the course of the magnetic study, there were difficulties in obtaining reproducible data. In addition, the values of the magnetic moments of some samples were higher than one would expect for low-spin ferric ion. This suggested the possibility of loss of pyridine ligand. An equilibrium study of $Fe(TPP)N_3$ with pyridine, and other selected bases, in CH_2Cl_2 at room temperature was undertaken in order to quantitatively document the nature of this reaction.

Walker et al.[32] and LaMar et al.[33] have previously reported an equilibrium study of Fe(TPP)Cl with aromatic nitrogenous bases in several solvents. The reaction proceeds in two steps:

$$Fe(TPP)Cl + B \overset{K_1}{\rightleftharpoons} Fe(TPP)ClB \quad (1)$$

$$Fe(TPP)ClB + B \overset{K_2}{\rightleftharpoons} Fe(TPP)B_2^+Cl^- \quad (2)$$

In general, for Fe(TPP)Cl $K_2 \gg K_1$, so the overall reaction

$$Fe(TPP)Cl + 2B \overset{\beta_2}{\rightleftharpoons} Fe(TPP)B_2^+Cl^-$$

where $\beta_2 = K_1K_2$ is usually observed. The complex Fe(TPP)Cl is five-coordinate with high-spin ferric ion. $Fe(TPP)B_2^+Cl^-$ is an associated ion pair; the complex cation is six-coordinate with low-spin ferric ion. The spin state and coordination of the ferric ion in Fe(TPP)ClB are not known. Below we compare the reactions of Fe(TPP)Cl with those of $Fe(TPP)N_3$.

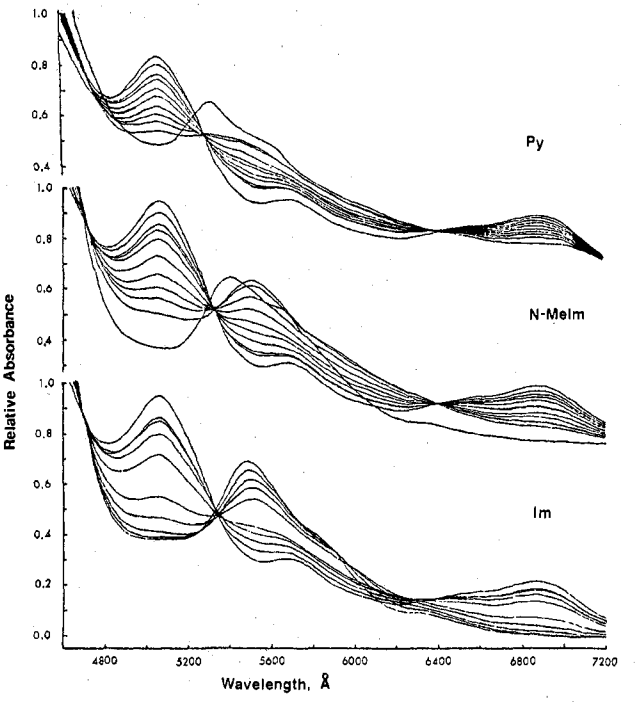

Figure 5. Visible spectral changes for the addition of selected bases to a solution of ~7 × 10^{-5} M $Fe(TPP)N_3$ in CH_2Cl_2.

The method used to determine the equilibrium constants was similar to that used by Walker et al.[32] Visible spectral changes were recorded as an increasing amount of the selected base was added to a solution with an initial concentration of ~7 × 10^{-5} M $Fe(TPP)N_3$ in CH_2Cl_2. These spectral changes are shown in Figure 5. When no base is present, absorption maxima are observed at 5060 and 6840 Å. As base is added, there is a gradual decrease in absorbance at these wavelengths; this is characteristic of a six-coordinate ferric porphyrin.[34,35] Isosbestic points are observed near 5320 and 6400 Å for the pyridine and *N*-methylimidazole cases; the spectra associated with large base excesses (i.e., pure base with the stock porphyrin solution) do not go through the isosbestic points. For the imidazole case the curves cross over but no isosbestic points were observed. Thus, in the case of pyridine and *N*-methylimidazole, it is likely that a single base is adding to $Fe(TPP)N_3$ until a large excess of base is present, at which point the equilibrium is driven toward the addition of a second base. For imidazole, the equilibrium reactions shift gradually from the addition of one base to two bases. The equilibrium constants calculated below support this interpretation.

The equilibrium constants were initially calculated by following the method of Walker et al.[32] The log $[(A_0 - A)/(A - A_c)]$ vs. log $[B]_0$ is plotted, where A is the relative absorbance at 5060 Å, A_0 is with no base present, A_c is with excess base, and $[B]_0$ is the initial concentration of base. With this method, if one base adds to the porphyrin, the plot should yield a straight line with a slope of 1.0; if two bases add, the slope should be 2.0. The log K_1 and log β_2 are the y intercepts of plots with slopes of 1.0 and 2.0, respectively.

Table XI gives the slopes and equilibrium constants calculated from a weighted linear least-squares fit of these plots. The slopes, particularly in the cases of pyridine and *N*-methylimidazole, show unacceptable deviations from 1.0 due to systematic errors. These errors arise from (1) the assumption that the extinction coefficients of $Fe(TPP)N_3B$ and $Fe(TPP)B_2^+N_3^-$ are the same at 5060 Å and (2) the large values of the K_1's compared to the K_2's. The former source of error is the same assumption Walker et al.[32] made with Fe(TPP)Cl; since $K_1 \ll K_2$ for the chloride derivative, any

Table XI. Parameters[a] from Least-Squares Fit of log $[(A_0 - A)/(A - A_c)]$ vs. log $[B]_0$ and the Resulting[b] Equilibrium Constants, K

base	slope	y intercept = log K	resulting K[b]	range of K
py	1.27 ± 0.10	0.51 ± 0.05	$K_1 = 3.2\ M^{-1}$	2.9–3.6 M^{-1}
N-MeIm	0.90 ± 0.08	1.85 ± 0.17	$K_1 = 71\ M^{-1}$	48–104 M^{-1}
Im	0.89 ± 0.24	1.90 ± 0.65	$K_1 = 79\ M^{-1}$	18–178 M^{-1}
	2.4 ± 1.6	5.2 ± 3.0	$\beta_2 = 1.6 \times 10^5\ M^{-2}$	160–1.6 × 10^8 M^{-2}

[a] Errors assigned to the parameters for py and *N*-MeIm are the 95% confidence intervals calculated from a least-squares fit of the nine data points; both fits gave 99.9% confidence of linear correlation. For imidazole, there are four and three data points, respectively, for the two least-squares lines; errors in this case are standard deviations because of the limited number of data, and values for the K's should only be considered rough estimates. [b] More accurate values for K_1 are 1.75 M^{-1} for py and 145 M^{-1} for *N*-MeIm; see text.

Table XII. Equilibrium Constants for Addition of Amines to Fe(TPP)Cl and Fe(TPP)N_3

		In CH_2Cl_2			
Fe(TPP)N_3	py	$K_1 = 1.75\ M^{-1}$ ($3.2\ M^{-1}$)[a]	Fe(TPP)Cl	*N*-MeIm	$K_1 = 88\ M^{-1}$, $\beta_2 = 1.0 \times 10^4\ M^{-2}$
Fe(TPP)N_3	*N*-MeIm	$K_1 = 145\ M^{-1}$ ($71\ M^{-1}$)[a]	Fe(TPP)Cl	Im	$\beta_2 = 4.8 \times 10^5\ M^{-2}$
Fe(TPP)N_3	Im	$K_1 = 79\ M^{-1}$ [a], $\beta_2 = 1.6 \times 10^5\ M^{-2}$ [a]			
		In $CHCl_3$			
Fe(TPP)Cl	py	$K_1 = \sim 0.2\ M^{-1}$, $\beta_2 = \sim 0.5\ M^{-2}$	Fe(TPP)Cl	*N*-MeIm	$K_1 = 9\ M^{-1}$, $\beta_2 = 1.50 \times 10^3\ M^{-2}$
			Fe(TPP)Cl	Im	$\beta_2 = 1.58 \times 10^6\ M^{-2}$

[a] Values calculated in a method similar to that used for chloride derivatives; inaccurate K's resulted for azide; see text.

systematic errors caused by this were negligible. To overcome these systematic errors, we must calculate the equilibrium constants by a method that does not use the absorbance in excess base, A_c.

A method that fits this criterion is the Benesi–Hildebrand method.[36] In using this method, we obtain a plot of $[B]_0/(A_0 - A)$ that is a straight line with the y intercept equal to $-1/K_1$. The plots for pyridine and *N*-methylimidazole gave a 99.9% confidence of linear correlation. The following equilibrium constants and 95% confidence intervals were calculated: K_1(py) = 1.75 M^{-1} (1.52–2.08 M^{-1}), K_1(*N*-MeIm) = 145 M^{-1} (132–161 M^{-1}). For imidazole, values of K_1 and β_2 could not be determined because of the two competing equililbria.

Table XII lists the equilibrium constants calculated for Fe(TPP)N_3 and those recorded elsewhere[32] for Fe(TPP)Cl. From this table it can be seen that for Fe(TPP)N_3 the reaction forming the mono(base) adduct, which is six-coordinate for the azide derivative, predominates, and for Fe(TPP)Cl the bis adduct is generally observed. This is attributed to the azide being a stronger base than the chloride.

The K_1's for Fe(TPP)N_3 decrease with decreasing basicity of the amine.[37] The K_2's do not show this correlation for Fe(TPP)N_3 or for Fe(TPP)Cl. In both cases K_2 for imidazole is much larger than K_2 for *N*-methylimidazole. This has been discussed by Walker et al.[32] The driving force for the overall reaction is presumably the stabilization of the ion pair Fe(TPP)$B_2^+X^-$. With imidazole the displaced anion can have a strong electrostatic interaction with the N–H bond of one of the imidazole ligands. The interaction weakens the N–H bond and further stabilizes the complex through delocalization of the positive charge on the iron to the imidazole. Walker et al.[32] have also suggested possible biological occurrence of this process of weakening the N–H bond of imidazole in hemoglobin and other hemoproteins. Sweigart[38] has recently observed, via spectroscopic measurement, a K_1 of 9.5 M^{-1} for reaction 1 with *N*-propylimidazole and Fe(TPP)Cl.

The low value of the equilibrium constant for the addition of pyridine to Fe(TPP)N_3 confirms the apparent instability of the pyridine bond suggested by the early (and nonreproducible) magnetic measurements. The molecular structure of Fe(TPP)N_3py·$^1/_2$py, which reveals a relatively long Fe–N_{py} bond owing to steric interaction of the pyridine hydrogen atoms with the porphinato core, is also consistent with an unstable pyridine bond. This study demonstrates that, for appropriate choices of the axial anionic and nitrogenous ligands, isolable unsymmetrically substituted ferric porphyrins can be obtained.

Acknowledgment. K.H. and W.R.S. gratefully acknowledge support from the National Institutes of Health through Grant HL-15627.

Registry No. Fe(TPP)N_3py·$^1/_2$py, 70046-79-6; Fe(TPP)N_3(*N*-MeIm), 70046-81-0; Fe(TPP)N_3Im, 70046-82-1; Fe(TPP)$Im_2^+N_3^-$, 70046-83-2; Fe(TPP)Cl, 16456-81-8.

Supplementary Material Available: A listing of structure factor amplitudes (20 pages). Ordering information is given on any current masthead page.

References and Notes

(1) (a) University of Michigan. (b) University of Notre Dame.
(2) J. L. Hoard, *Science*, **174**, 1295 (1971).
(3) K. M. Smith, Ed., "Porphyrins and Metalloporphyrins", Elsevier, New York, 1975; C. A. McAuliffe, Ed., "Techniques and Topics in Bioinorganic Chemistry", Wiley, New York, 1975.
(4) S. Peng and J. A. Ibers, *J. Am. Chem. Soc.*, **98**, 8032 (1976).
(5) J. P. Collman, T. N. Sorrell, K. O. Hodgson, A. K. Kulshrestha, and C. E. Strouse, *J. Am. Chem. Soc.*, **99**, 5180 (1977).
(6) A. D. Adler, F. R. Longo, F. Kampas, and J. Kim, *J. Inorg. Nucl. Chem.*, **32**, 2443 (1970).
(7) W. L. Jolly, "The Synthesis and Characterization of Inorganic Compounds", Prentice-Hall, Englewood Cliffs, N.J., 1970, pp 116–21.
(8) K. M. Adams, Ph.D. Thesis, University of Michigan, Ann Arbor, Mich., 1977, pp 59, 84–7.
(9) W. R. Scheidt, DIFFDAT, University of Notre Dame, Notre Dame, Ind., 1970.
(10) W. R. Scheidt, *J. Am. Chem. Soc.*, **96**, 84 (1974).
(11) (a) P. W. R. Corfield, R. J. Doedens, and J. A. Ibers, *Inorg. Chem.*, **6**, 197 (1967); (b) W. R. Busing and H. A. Levy, *J. Chem. Phys.*, **26**, 563 (1957).
(12) J. M. Stewart, X-RAY 72, TR-192, University of Maryland, College Park, Md., 1967.
(13) C. H. MacGillavry, G. D. Reich, and K. Lonsdale, "International Tables for X-Ray Crystallography", Vol. III, Kynoch Press, Birmingham, England, 1962, pp 201–9.
(14) J. A. Ibers and W. C. Hamilton, "International Tables for X-Ray Crystallography", Vol. IV, Kynoch Press, Birmingham, England, 1974, pp 148–51.
(15) J. W. Schilling, "Crystallographic Computing", F. R. Ahmed, Ed., Copenhagen, Munksgaard, 1970, pp 201–4.
(16) M. R. Churchill, *Inorg. Chem.*, **12**, 1213 (1973).
(17) R. F. Stewart, E. Davidson, and W. Simpson, *J. Chem. Phys.*, **42**, 3175 (1965).
(18) C. K. Johnson, "ORTEP", Report ORNL-3794, Oak Ridge National Laboratory, Oak Ridge, Tenn., 1965.
(19) J. L. Hoard, *Ann. N.Y. Acad Sci.*, **206**, 18 (1973).
(20) D. M. Collins, R. Countryman, and J. L. Hoard, *J. Am. Chem. Soc.*, **94**, 2066 (1972).
(21) A. Takenaka, Y. Sasada, E. Watanabe, H. Ogoshi, and Z. Yoshida, *Chem. Lett.*, 1235 (1972).
(22) W. R. Scheidt and J. L. Hoard, unpublished results.
(23) L. J. Radonovich, A. Bloom, and J. L. Hoard, *J. Am. Chem. Soc.*, **94**, 2073 (1972).

(24) J. A. Kaduk and W. R. Scheidt, *Inorg. Chem.*, **13**, 1875 (1974).
(25) W. R. Schiedt, J. A. Cunningham, and J. L. Hoard, *J. Am. Chem. Soc.*, **95**, 8289 (1973).
(26) W. R. Scheidt, *J. Am. Chem. Soc.*, **96**, 90 (1974).
(27) C. Maricondi, W. Swift, and D. K. Straub, *J. Am. Chem. Soc.*, **91**, 5205 (1969).
(28) L. M. Epstein, D. K. Straub, and C. Maricondi, *Inorg. Chem.*, **6**, 1720 (1967).
(29) B. N. Figgis, "Introduction to Ligand Fields", Wiley, New York, 1966, pp 248–292.
(30) F. E. Mabbe and D. J. Machin, "Magnetism and Transition Metal Complexes", Chapman and Hall, London, 1973, pp 110–120.
(31) G. Harris, *Theor. Chim. Acta*, **10**, 119 (1968).
(32) F. A. Walker, M. Lo, and M. T. Ree, *J. Am. Chem. Soc.*, **98**, 5552 (1976).
(33) J. D. Satterlee, G. N. LaMar, and J. S. Frye, *J. Am. Chem. Soc.*, **98**, 7275 (1976).
(34) P. George, J. Beetlestone, and J. S. Griffith, "Haematin Enzymes", Pergamon Press, New York, 1961, p 111.
(35) H. Kobayashi, Y. Yanagawa, H. Osada, S. Minami, and M. Shimizu, *Bull. Chem. Soc. Jpn.*, **46**, 1471 (1973).
(36) R. Foster, "Organic Charge-Transfer Complexes", Academic Press, New York, 1969, pp 126–39.
(37) $pK_a(BH^+)$: py, 5.25 M; *N*-MeIm, 6.95 M; Im, 6.95 M [R. C. Weast, Ed., "CRC Handbook of Chemistry and Physics", 55th ed., CRC Press, Cleveland, Ohio, 1974–1975, p D-127].
(38) D. A. Sweigart and D. Burdige, *Inorg. Chim. Acta*, **28**, L131 (1978).

Contribution from the Department of Chemistry, University of Colorado, Boulder, Colorado 80309

Structural Characterization of *trans*-2,4-Dithio-2,4-dianilino-1,3-diphenyl-1,3,2,4-diazadiphosphetidine, $[(C_6H_5NH)P(S)NC_6H_5]_2$

CHUNG-CHENG CHANG, R. CURTIS HALTIWANGER, MARTIN L. THOMPSON, HAW-JAN CHEN, and ARLAN D. NORMAN*[1]

Received December 6, 1978

Reaction of β-$P_4S_3I_2$ with aniline results in formation of $[(C_6H_5NH)P(S)NC_6H_5]_2$, I, in moderate yield. The structure of I has been established by spectral data and a single-crystal X-ray analysis as *trans*-2,4-dithio-2,4-dianilino-1,3-diphenyl-1,3,2,4-diazadiphosphetidine. I forms monoclinic crystals in space group $P2_1/c$ with a = 15.287 (5) Å, b = 8.639 (2) Å, c = 18.728 (5) Å, β = 108.97 (2)°, Z = 4, d_{obsd} = 1.39 g cm^{-3}, d_{calcd} = 1.398 g cm^{-3} (20 °C, Mo Kα). The structure, solved by direct methods, refined to R_f = 0.062 and R_{wF} = 0.064 for 2127 independent observed reflections. The unit cell of I contains molecules of two slightly different conformational types, A and B, of C_i and approximate C_{2h} symmetries, respectively. The mean ring P—N, exocyclic P—N, and P=S distances are 1.688 (8), 1.670 (6), and 1.905 (4) Å, respectively. The mean ring P–N–P, ring N–P–N, and *exo*-S–P–N angles are 101.2 (3), 108.5 (4), and 102.3 (3)°, respectively. Comparison of $[(C_6H_5NH)P(S)NC_6H_5]_2$ from $(C_6H_5NH)_3PS$ thermolysis with I from the β-$P_4S_3I_2$–$C_6H_5NH_2$ reaction indicates that the two are identical. There is no evidence for cis isomeric product in either reaction system. From the reaction of α-$P_4S_3I_2$ with $C_6H_5NH_2$, traces of $[(C_6H_5NH)P(S)NC_6H_5]_2$ of a possibly different structural form than I are obtained.

Introduction

The reactions of aniline with α- or β-$P_4S_3I_2$ have been reported recently to yield compound(s) of formula $[(C_6H_5NH)P(S)NC_6H_5]_2$, in addition to a series of (phenylimido)- and sulfidotetraphosphorus ring and cage compounds.[2] The $[(C_6H_5NH)P(S)NC_6H_5]_2$ is a major recoverable product of the β-$P_4S_3I_2$–$C_6H_5NH_2$ reaction; however, it is present only as a trace product in the α-$P_4S_3I_2$–$C_6H_5NH_2$ system. Although spectral data indicated tentatively that the products are 2,4-dithio-1,3,2,4-diazadiphosphetidine(s)

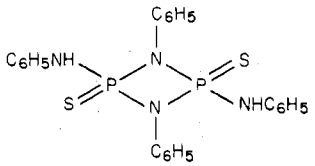

in either or both of the cis and trans isomeric forms, structural characterization remained indefinite.

Single-crystal X-ray studies of dithiodiazadiphosphetidines of type $[RP(S)NR']_2$ (R = C_6H_5, R' = CH_3, C_2H_5, C_6H_5)[3-6] and correlation of their spectral data with cis and trans structural features have been reported.[6,7] Similar structural studies of the more interesting RNH-containing $[(RNH)P(S)NR]_2$ compounds have not appeared. Therefore, in order to establish unequivocally the structures of products from the β-$P_4S_3I_2$–aniline reactions and to establish structural bases for spectral correlation and for further syntheses, we carried out a single-crystal study of $[(C_6H_5NH)P(S)NC_6H_5]_2$ from the β-$P_4S_3I_2$–$C_6H_5NH_2$ reaction. In addition, a comparative study of this product with $[(C_6H_5NH)P(S)NC_6H_5]_2$ from $(C_6H_5NH)_3PS$ thermolysis,[8] which also has not been structurally characterized, has been effected.

Experimental Section

Apparatus and Materials. All inert-atmosphere manipulations were carried out in N_2-flushed glovebags and standard Schlenk-type glassware.[9] Infrared spectra (4000–400 cm^{-1}) were obtained by using Perkin-Elmer 337G and Beckman Model IR-12 spectrophotometers. High-resolution mass spectra were obtained by using an AEI MS-9 spectrometer at The Pennsylvania State University. Proton nuclear magnetic resonance spectra were collected at 90.0 Hz by using a Varian EM 390 spectrometer and at 100.0 MHz by using a JEOL-PFT 100 Fourier transform spectrometer. Both were equipped with standard variable-temperature probe accessories. Proton chemical shifts were measured relative to internal $(CH_3)_4Si$; chemical shifts downfield from the standard are given positive (+δ) values. ^{31}P NMR spectra were obtained by using the JEOL-PFT 100 Fourier transform spectrometer equipped with standard 40.5-MHz probe accessories. ^{31}P chemical shifts were measured relative to external 85% H_3PO_4. Chemical shifts downfield from the standard are given negative (–δ) values. Spectral simulation and the calculation of spectral parameters for second-order spectra were accomplished by using a Nicolet 1080 Series NMR spectrum calculation program, NMRCAL NIC-801S-7117D, Nicolet Instrument Corp., Madison, Wis. Single-crystal X-ray data were collected at ambient temperature by using a Syntex $P\bar{1}$ automated diffractometer equipped with a graphite monochromator.

$(C_6H_5NH)_3PS$,[8] α-$P_4S_3I_2$,[10] and β-$P_4S_3I_2$[11,12] were prepared as reported earlier. Toluene was dried over $LiAlH_4$, CS_2 over P_4O_{10}, and $CHCl_3$ over P_4O_{10} before use. Ethanol (Mallinckrodt, absolute) was used as obtained.

Reaction materials from the reactions below were characterized by comparison of their physical and/or spectral properties with those reported in the literature or with spectra of samples prepared independently in our laboratories. Mass spectral data, in the sections below, refer to the major peak in the envelope in question.

0020-1669/79/1318-1899$01.00/0